AQUATIC RESEARCH

AQUATIC RESEARCH
E-ISSN 2618-6365

Aquat Res 6(3), 201-226 (2023) • https://doi.org/10.3153/AR23020 *Research Article*

Assessing eutrophication vulnerability in Köyceğiz Lake: Climate change and basin developments impact trophic status

Elif ATASOY AYTIŞ[1], **Elif SOYER**[1], **Ali ERTÜRK**[2]

Cite this article as:
Atasoy Aytış, E., Soyer, E., Ertürk, A. (2023). Assessing eutrophication vulnerability in Köyceğiz Lake: Climate change and basin developments impact trophic status. *Aquatic Research*, 6(3), 201-226. https://doi.org/10.3153/AR23020

[1] Marmara University, Faculty of Engineering, Department of Environmental Engineering, Istanbul, Türkiye

[2] Istanbul University, Faculty of Aquatic Sciences, Department of Freshwater Resources Management, Istanbul, Türkiye

ORCID IDs of the author(s):
E.A.A. 0000-0001-9097-181X
E.S. 0000-0003-1400-5198
A.E. 0000-0002-3532-2961

ABSTRACT

This study investigated the potential for eutrophication in Köyceğiz Lake, one of Türkiye's most important and sensitive ecosystems. We developed a simple steady-state eutrophication model system using a phosphorus mass balance model for the lake, utilising open-access data from the literature as input. The model was calibrated and validated, with a specific focus on the eutrophic state of Köyceğiz Lake, and it demonstrated good responsiveness to future predictions. Our findings revealed that both the epilimnion (TSI (TP) 56) and hypolimnion (TSI (TP) 70) of Köyceğiz Lake are eutrophic. Considering climate change impacts and developments in the basin, we conducted projections to determine the lake's trophic status between 2035 and 2095. By 2035, a 65% decrease in freshwater inflow and a 4% increase in total TP load will lead to a hypertrophic status, which will persist and gradually worsen to a severe trophic situation by 2095.

Keywords: Climate change, Diffuse pollution, Eutrophication, Köyceğiz Lake, Phosphorus

Submitted: 16.06.2023
Revision requested: 26.06.2023
Last revision received: 04.07.2023
Accepted: 10.07.2023
Published online: 12.07.2023

Correspondence:
Elif ATASOY AYTIŞ
E-mail: atasoy.e@gmail.com

Available online at
http://aquatres.scientificwebjournals.com

Introduction

The surface waters face two significant challenges: (i) the impact of climate change and (ii) the inability to control diffuse pollution sources effectively. Climate change has emerged as a crucial factor affecting freshwater resources over the past three decades, with meteorological and climatological events playing a prominent role (Şen, 2020). Despite the constancy of global water resources within the water cycle, managing water quantity and quality has become increasingly difficult in numerous locations due to changes in precipitation patterns, surface runoff, and groundwater recharge worldwide (Görgüner et al., 2019). According to the IPCC Sixth Assessment Report (IPCC, 2022), the current 1.1°C warmer world has led to more frequent heatwaves and droughts, with projected negative impacts on southern regions of Europe. In the Western Mediterranean Region of Türkiye, temperatures have risen, surpassing the country's average, accompanied by a decrease in annual and winter precipitation since the 1960s. Consequently, the adverse effects of climate change on freshwater resources and the water budget in this region are inevitable (Şen, 2013; Ertürk et al., 2014).

In the past two decades, the effectiveness of legislation and regulations in addressing point source pollution in surface water systems has increased, resulting in faster and easier mitigation measures. However, to further enhance water quality and ensure compliance with water quality regulations, it is crucial to identify and measure the sources of diffuse pollution (DEFRA, 2002). Agricultural-derived nutrient pollution is the most significant factor in water quality degradation in the USA (Buckley and Carney, 2013). While there have been recent improvements in water quality in European Union countries, many aquatic ecosystems remain at risk of eutrophication due to excessive concentrations of nitrogen (N) and phosphorus (P) (Udias et al., 2016). According to the National Lakes Assessment Report, 20% of the 50,000 lakes examined are impacted by nitrogen and phosphorus pollution (NAO, 2010).

The Turkish economy is primarily based on agriculture and livestock activities. Diffuse source pollution accounts for more than half of the total pollution loads, leading to eutrophication issues in surface waters (Ayaz et al., 2021; 2022).

This study aims to initiate efforts to establish a simple eutrophication model system for a natural lake. In this context, our contributions can be summarised as follows: (i) illustrating the lake's responses to future predictions and (ii) creating a valuable tool for addressing various nutrient management and climate change simulations. We have selected the Köyceğiz Lake basin as our case study area to achieve this. Köyceğiz Lake, located in the western Mediterranean region of Türkiye, is part of a complex lagoon system known as the Köyceğiz-Dalyan Lagoon. This system is predominantly composed of brackish water. Considering this characteristic and the lake's classification as a meromictic lake (Kazancı et al., 1992; Bayarı et al., 1995), investigating the lake presents an intriguing task. In recent decades, numerous studies have been conducted on lagoon systems (Gürel, 2000; Ertürk, 2002; Tanık et al., 2005; Ekdal, 2008; Balloch, 2009; Ertürk et al., 2014; Güzel, 2020). Recently, Keskin (2019) conducted a study on the eutrophication risk in a lagoon system and determined that total phosphorus (TP) is the limiting nutrient in Köyceğiz Lake. Another study by Taşeli (2017), based on a four-year monthly monitoring scheme from 2008 to 2011, calculated TN/TP ratios greater than 20, leading to the conclusion that TP is the limiting nutrient in the lake according to the Vollenweider model (Vollenweider, 1976). The factors influencing the limiting nutrients in the lake include the loads transported through the basin by the streams and the nutrient content of the Eastern Mediterranean Sea (Levantine Basin). The Eastern Mediterranean Sea exhibits a TN/TP mass ratio ranging from 25 to 28, resulting in severe phosphorus limitation for primary productivity in the Eastern basin (Krom et al., 1991; Kress and Herut, 2001; Krom et al., 2005; Koçak et al., 2010; Lazzari et al., 2016). The TN and TP loads calculated by Tanık et al. (2005) indicate an approximate TN to TP load ratio of 13, further confirming that phosphorus is the limiting nutrient in Köyceğiz Lake.

These studies and several others not mentioned here clearly indicate that no ecological model has been developed for Köyceğiz Lake, the largest waterbody in the system. Our model aims to examine the eutrophication status of the lake and employs a mechanistic modelling approach.

Material and Methods

Site Description

Köyceğiz Lake, which is part of the Dalyan Lagoon system, is a natural, meromictic lake located on the southwest coast of

Türkiye, adjacent to the Mediterranean Sea (Kazancı et al., 1992; Bayarı et al., 1995). The key morphological parameters describing the lake are presented in Table 1. It is a moderately-sized lake, measuring 13 km in length, 2-6 km in width, with an average depth of 25 m. The lake has a surface area of 55 km^2. Based on salinity profile analysis, the boundary between the upper layer (epilimnion) and lower layer (hypolimnion) was determined at a depth of 6.5 m (Ertürk, 2002). Monitoring studies in the lake indicate that the average salinity of the epilimnion and hypolimnion is approximately 3 ppt and 10 ppt, respectively (Gürel, 2000; Özgül, 2015; Karaca, 2020).

The lake collects surface water from 1011 km^2 (Figure 1-a). The principal streams that discharge into the lake are Namnam Creek, Yuvarlak Creek, and Kargıcak Creek, with drainage areas of 604 km^2, 105 km^2, and 43 km^2, respectively.

According to TurkStat (a) (2018), the basin's population was 37,618 people. The basin encompasses three districts: Köyceğiz, Ula, and Ortaca (Figure 1-b). Among these, 86% of the population of the Köyceğiz district and 25% of the Ula district are located within the basin. In terms of area, the Köyceğiz district accounts for 63% of the basin, while the Ula district comprises 27%. The remaining part is represented by Menteşe (5%) and Ortaca (4%) districts, which have a relatively small area.

The land use distribution in the basin consists of 52% forest, 30% meadow and pasture, 17% agricultural areas, and 1% other areas, including settlements (CORINE, 2018) (Figure 2).

Due to its unique and significant ecosystem with a high species diversity, the lake and its basin were designated as a Special Environmental Protection Area (SEPA) by the Turkish Government in 1988.

The basin experiences a typical Mediterranean climate with hot and dry summers and mild and rainy winters.

Hydrological Investigation

The lake's water budget, crucial for modelling studies, was obtained from a previous study by Ertürk et al. (2014). In that study, the anticipated impact of climate change on the watershed was quantified at the hydrological process level. A hydrological model was developed using SWAT, which was calibrated and validated. Over the years, the average total flow derived from this hydrological model was used to determine the total surface runoff entering the lake from the basin. The calculated amount of water reaching the lake from the basin was 23.63 $m^3 s^{-1}$. Estimations of future freshwater inflow were performed using the basin's water yield trend equation (mm/yr), as provided in Ertürk et al. (2014).

Estimation of Phosphorus Loads

Given that TP is the limiting nutrient in the lake (Taşeli, 2017; Keskin, 2019), all calculations were explicitly conducted for TP. The calculations of TP pollution loads were performed for the years 1990, 2000, 2006, 2012, and 2018, corresponding to the availability of CORINE land cover data. These calculations aimed to illustrate past trends and determine potential future scenarios without any nutrient load mitigation measures.

Table 1. Characterising parameters of the lake

Parameter (unit)	Abbreviation	Köyceğiz Lake
Area (km^2)	A	55
Volume of epilimnion (10^6 m^3)	V_E	356.6
Volume of hypolimnion (10^6 m^3)	V_H	389.6
Height of epilimnion (m)	H_E	6.5
Height of hypolimnion (m)	H_H	11.1
The salinity of epilimnion (ppt)	S_E	3
Salinity of hypolimnion (ppt)	S_H	10

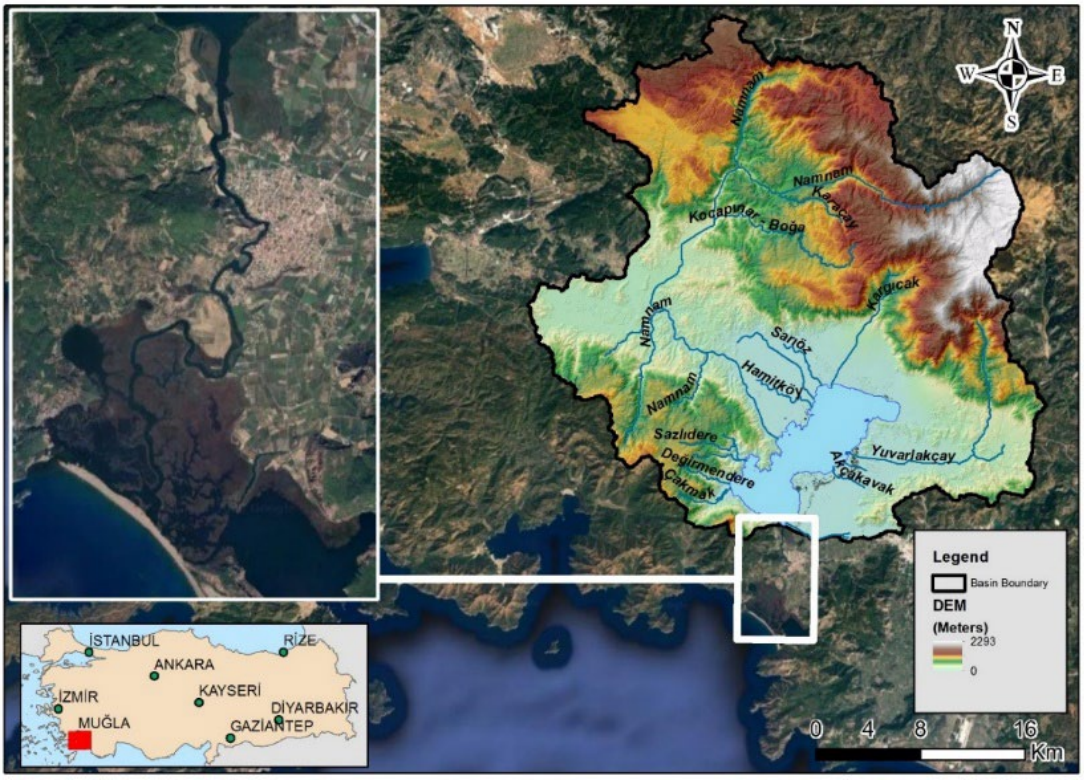

(a)

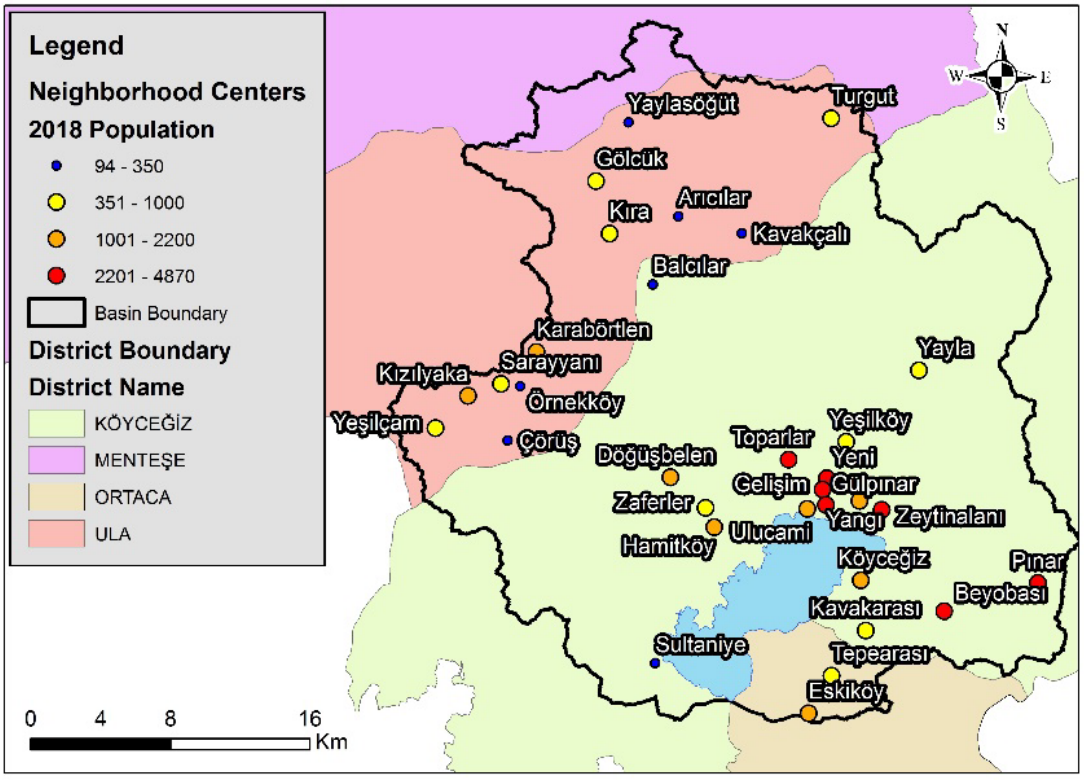

(b)

Figure 1 Geographic map of the basin (a) administrative borders of the basin (b)

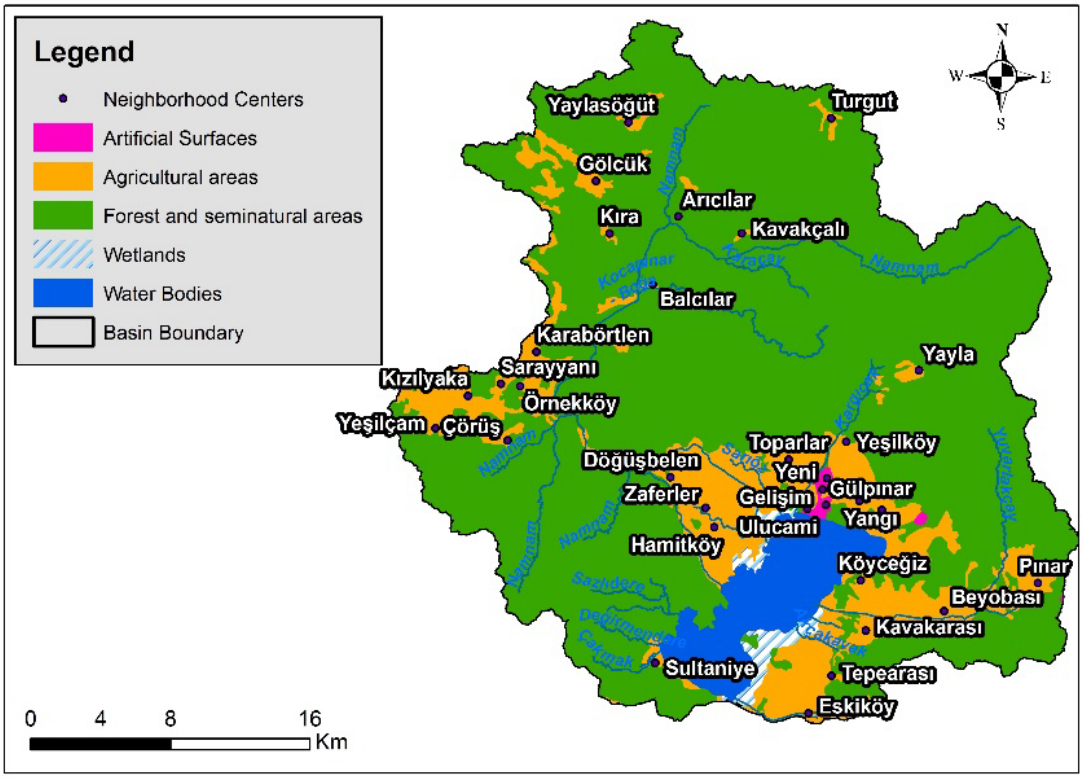

Figure 2. CORINE 2018 land cover map of the basin

Since 2002, a municipal wastewater treatment plant with nutrient (nitrogen and phosphorus) removal has been operational, treating wastewater from 95% of the population. Additionally, there have been no industrial discharges in the basin. It can be assumed that nutrient emissions primarily originate from diffuse sources. Although the wastewater treatment plants effectively treat nutrients, a certain amount of TP load is still discharged into the lake through the effluent. The TP input from the municipal wastewater treatment plant was calculated considering the TP removal performance of the plant, the basin's population, the annual volume of treated wastewater, and the treatment plant's capacity.

In this study, the primary diffuse pollutant sources in the basin were classified as land use, agricultural activities (fertiliser usage), and livestock activities (Figure 3). The calculations were conducted by considering the unit loads and emissions of TP obtained from the literature (Table 2). Climatic conditions, soil characteristics, population trends, agricultural practices, and cultural factors significantly influence the unit loads. The unit loads for each pollution source were selected based on studies conducted in Türkiye (Gürel et al., 2011; Ayaz et al., 2013; MoAF, 2018).

The land use distribution and the respective area values for each land use activity were determined using the CORINE land cover data. To estimate the loads originating from land usage (natural activities), the following unit loads were utilised: 0.05 kg TP/ha-year for forests, 0.1 kg TP/ha-year for meadows, 0.5 kg TP/ha-year for urban areas, and 0.90 kg TP/ha-year for rural areas (Gürel et al., 2011).

The yearly chemical fertiliser application data, measured in kg $P_2 0_5$/ha-year for different crop types, were obtained from the Fertilizer Recommendation Guideline published by the Ministry of Agriculture and Forestry (MoAF, 2018). These data were then evaluated with the corresponding years' CORINE land cover data.

The number of livestock, including bovines and ovines, was acquired from TurkStat (b) between 2004 and 2018. The animal unit loads were multiplied by the weight of the animals to estimate the animal-based TP loads. For bovines, a unit load of 18 kg TP/animal-year was used, while for ovines, a unit load of 1 kg TP/animal-year was applied (Ayaz et al., 2013).

Regarding fertiliser application and livestock-based loads, losses through leaching and surface runoff typically range from 0.5% to 5% of the land-based TP amount, depending on meteorological, climatic, geographical, and geological conditions (Gürel et al., 2011). Since a 2.5% TP loss rate was determined to be suitable for Türkiye (Ayaz et al., 2017), this ratio was utilised to calculate the TP amount reaching the receiving water in this study.

To estimate the future point and diffuse TP loads, it was assumed that the land use distribution and crop pattern would remain unchanged in the basin. However, the logistic curve method was employed to project the population, number of bovine livestock, and number of ovine livestock in the basin (for further details, refer to **Appendix A**).

Travel Time in The Streams

The movement and transformation of nutrients during stream transport must be considered, as nutrients are carried from land-based activities to lakes through streams. The travel time of nutrients in the streams was calculated to assess these conditions. To accomplish this, the Manning formula was utilised to formulate equations for the travel time of streams. The equation for stream travel time, along with its derivation, can be found in **Appendix B**. Consequently, the travel time (in hours) of nutrients along the streams was determined.

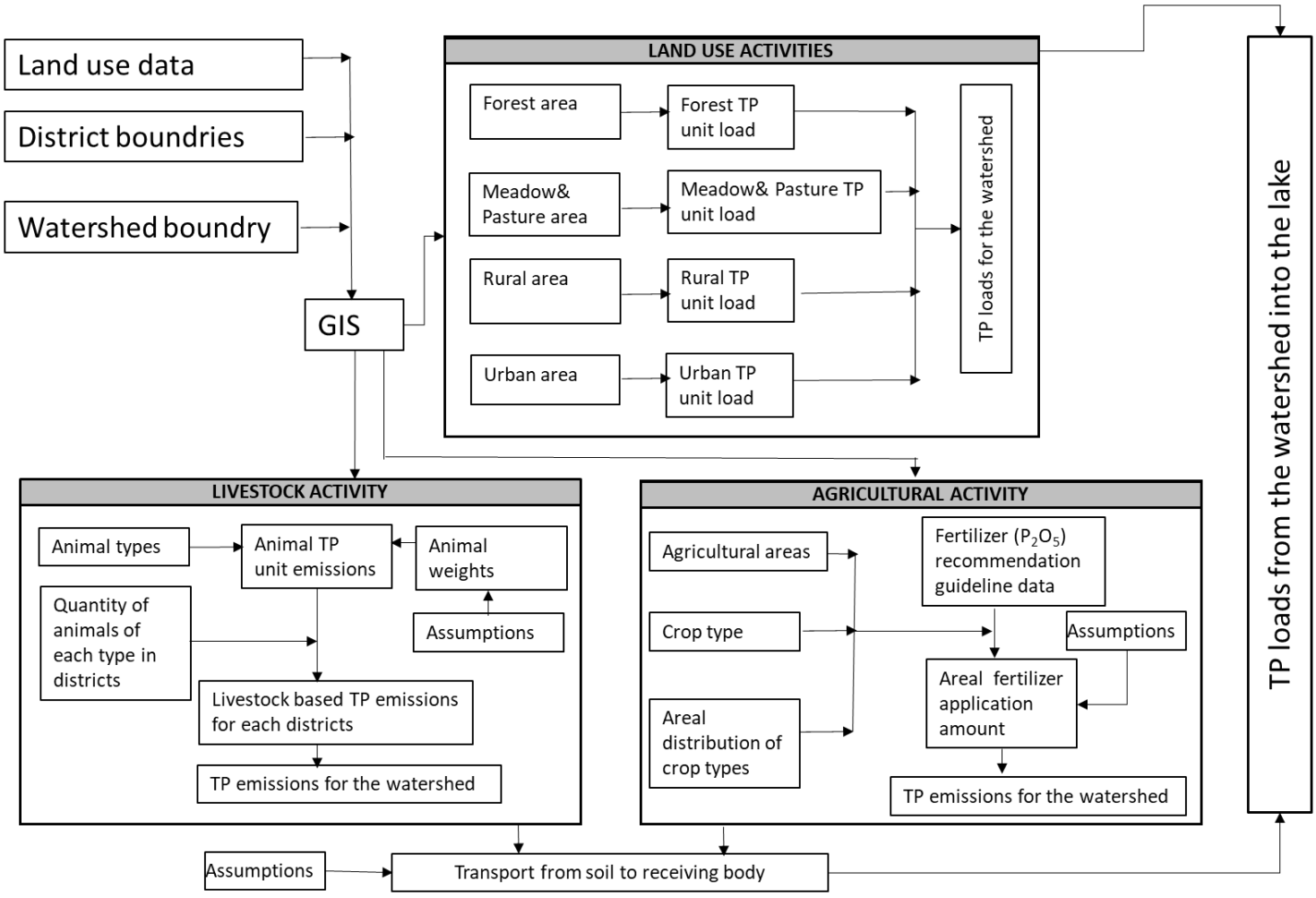

Figure 3. Methodology for estimation of diffuse TP pollution load

Table 2. Unit loads and emissions for estimation of diffuse TP pollution load

Pollution Source Activity	Unit Diffuse TP Loads	Unit Diffuse TP Emissions	From Soil to Receiving Body (Ayaz et al.2017)	Data Source	Reference
Land Use	**TP (kg/ha-year)**				
Forest	0.05				
Meadow and Pasture	0.1		-	CORINE	Gürel et al. 2011
Rural	0.90				
Urban	0.50				
Livestock		**TP (kg/animal-year)**			
Bovine (≈500 kg)		18	2.5 %	TurkStat	Ayaz et al., 2013
Ovine (≈45 kg)		1			
Agriculture		**P_2O_5 (kg P_2O_5/ha-year)***			
Olive grove		90			
Orchard- irrigated		120	2.5%	CORINE	MoAF, 2018
Orchard-not irrigated		80			
Crops-not irrigated		88			
Crops-irrigated		100			

*43% of P_20_5 amount is TP

The Lake Eutrophication Model System

The article aims to assess the trophic level of Köyceğiz Lake in its current state and examine the potential changes in trophic level over the next 10 years based on applied scenarios. However, our objective is not to examine the annual variations in the lake's condition. In Türkiye, the trophic level of a lake, mainly whether it is eutrophic or not, is determined according to the Carlson Index, as specified in the regulations (MoAF, 2021). To evaluate the impact of the applied scenarios on the lake, it is necessary to assess the changes in the Carlson Index. The Carlson Index calculates based on the average annual concentration values (Carlson 1977, Carlson and Simpson 1996) without making a seasonal distinction. Additionally, Köyceğiz Lake is a natural and mature lake, suggesting that it is in an equilibrium state even if there are seasonal fluctuations within the lake.

For these reasons, in this study, a simple eutrophication model was developed for Köyceğiz Lake using a steady-state approach, eliminating the need for dynamic modelling. The annual average TP concentrations were calculated for the epilimnion and hypolimnion layers using the steps described below.

Since water travel time in streams is generally within hours, the retention and transformation of nutrients in the streams were not considered in calculating diffuse TP loads at this study stage. Instead, the streams were regarded as conduits that collect and channel TP loads into the basin. Considering the meromictic nature of the lake, the developed model in this study consisted of two layers, namely the epilimnion and hypolimnion, characterised by stable stratification (Figure 4). The condition of the epilimnion and hypolimnion layers and the necessary morphological information for Köyceğiz Lake were obtained from Ertürk (2002).

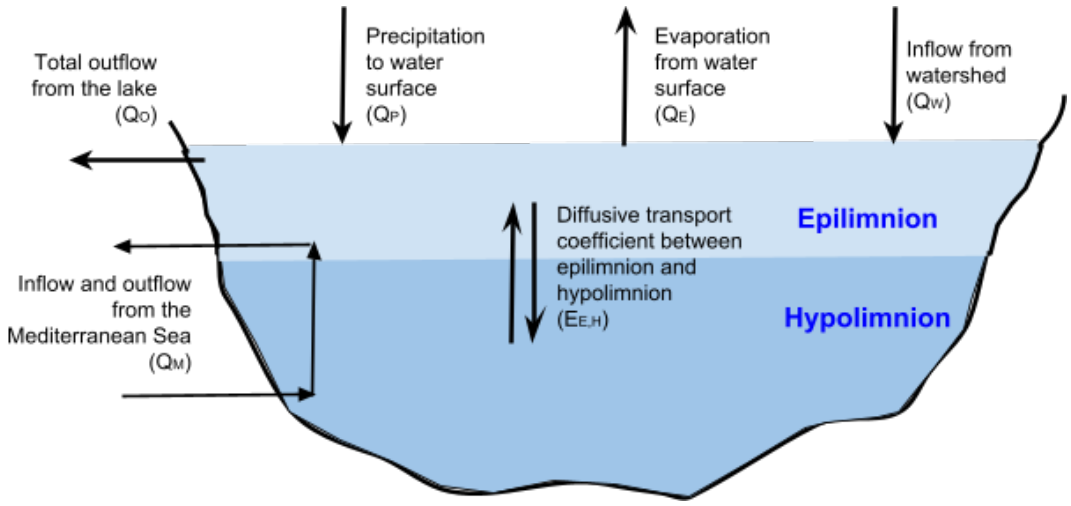

Figure 4. Schematic diagram of the lake

where

Q_W= Freshwater inflow rate of the lake (m^3 day^{-1}), Q_P=Precipitation to the water surface (m^3 day^{-1}), Q_E= Evaporation from water surface (m^3 day^{-1}), Q_M= Inflow from the Mediterranean Sea (m^3 day^{-1}), $Q_{O,E}$=Total outflow from the epilimnion (m^3 day^{-1}), $Q_{O,H}$=Total outflow from the hypolimnion (m^3 day^{-1}).

The estimation of the average annual inflow from the Mediterranean Sea into Köyceğiz Lake and the diffusive transport within the lake were conducted using the salt budget, based on data from Kazancı et al. (1992) and Bayarı et al. (1995) (details can be found in Appendix C). As mentioned earlier, TP was identified as the limiting nutrient in Köyceğiz Lake (Taşeli, 2017; Keskin, 2019). Considering this, the TP mass balance in the lake was solved using linear equations for the steady-state condition.

Monitoring data provided by Gürel (2000) indicated that the TP concentrations in the Mediterranean Sea were nearly the same at the surface and bottom of the Dalyan Channel. Considering this, the TP concentration entering the lake from the Mediterranean Sea through the Dalyan Channel was determined to be 65 µg L^{-1}, as reported in a recent study by Karaca (2020).

The mass balance equations for TP can be expressed as follows.

$$Q_{O,E} = Q_W + Q_P - Q_E + Q_M \quad (1)$$

$$Q_{O,H} = Q_M \quad (2)$$

$$\frac{dP_E}{dt} = -\left(\frac{Q_M + Q_{O,E}}{V_E} + \frac{\vartheta_{S,E}}{H_E}\right) \cdot P_E + \frac{Q_M}{V_E} \cdot P_H + \frac{W_{P,E}}{V_E} + \frac{E_{E,H} \cdot (P_H - P_E)}{V_E} \quad (3)$$

$$\frac{dP_E}{dt} = -\left(\frac{Q_M + Q_{O,E}}{V_E} + \frac{\vartheta_{S,E}}{H_E} + \frac{E_{E,H}}{V_E}\right) \cdot P_E + \left(\frac{Q_M + E_{E,H}}{V_E}\right) \cdot P_H + \frac{W_{P,E}}{V_E} \quad (4)$$

$$\frac{dP_H}{dt} = \frac{\vartheta_{S,E}}{H_E} \cdot \frac{A_{E,H}}{A_S} \cdot P_E - \left(\frac{Q_M}{V_H} + \frac{\vartheta_{S,H}}{H_H}\right) \cdot P_H + \frac{W_{P,H}}{V_H} + \frac{Q_M}{V_H} \cdot P_{M+} \frac{E_{E,H} \cdot (P_E - P_H)}{V_H} \quad (5)$$

$$\frac{dP_H}{dt} = \left(\frac{\vartheta_{S,E}}{H_E} \cdot \frac{A_{E,H}}{A_S} + \frac{E_{E,H}}{V_H}\right) \cdot P_E - \left(\frac{Q_M}{V_H} + \frac{\vartheta_{S,H}}{H_H} + \frac{E_{E,H}}{V_H}\right) \cdot P_H + \frac{W_{P,H}}{V_H} + \frac{Q_M \cdot P_M}{V_H} \quad (6)$$

where

P_E= TP concentration in epilimnion (μg L^{-1}), P_H= TP concentration in hypolimnion (μg L^{-1}), P_M= TP concentration of Mediterranean Sea (μg L^{-1}), $\upsilon_{S,E}$= Settling velocity of epilimnion layer (m d^{-1}), $\upsilon_{S,H}$= Settling velocity of hypolimnion layer (m d^{-1}), V_E= Volume of epilimnion layer (m^3), V_H= Volume of hypolimnion layer (m^3), H_E= Height of epilimnion layer (m), H_H= Height of hypolimnion layer (m), A_S=Surface are of the lake (m^2), $A_{E,H}$= Interface area between epilimnion and hypolimnion layers (m^2), $E_{E,H}$= Diffusive transport coefficient between epilimnion and hypolimnion layers (m^3 day^{-1}), $W_{P,E}$= Land-based loads into epilimnion (g m^{-3} d^{-1}), $W_{P,H}$= Land-based loads into hypolimnion (g m^{-3} d^{-1}).

At steady-state conditions, the following equations were derived using constant "a" for the transfer between the epilimnion and hypolimnion and between the hypolimnion and epilimnion:

$$a_{E,E} \cdot P_E + a_{E,H} \cdot P_H + W'_{P,E} = 0 \quad (7)$$

$$a_{H,E} \cdot P_E + a_{H,H} \cdot P_H + W'_{P,E} + W'_M = 0 \quad (8)$$

If we express it in matrix form and then multiply both sides by -1 (inverting the matrix), we obtain our system matrix and the constant vector.

$$\begin{bmatrix} a_{E,E} & a_{E,H} \\ a_{H,E} & a_{H,H} \end{bmatrix} \begin{bmatrix} P_E \\ P_H \end{bmatrix} = -\left(\begin{bmatrix} W'_{P,E} \\ W'_{P,H} \end{bmatrix} + \begin{bmatrix} 0 \\ W'_M \end{bmatrix} \right) \quad (9)$$

$$W'_{P,E} = W'_{T,PE} \quad (10)$$

$$W'_{P,H} + W'_M = W'_{T,PH} \quad (11)$$

$$\begin{bmatrix} a_{E,E} & a_{E,H} \\ a_{H,E} & a_{H,H} \end{bmatrix} \begin{bmatrix} P_E \\ P_H \end{bmatrix} = -\begin{bmatrix} W'_{T,PE} \\ W'_{T,PH} \end{bmatrix} \times (-1) \quad (12)$$

$$\begin{bmatrix} -a_{E,E} & -a_{E,H} \\ -a_{H,E} & -a_{H,H} \end{bmatrix} \begin{bmatrix} P_E \\ P_H \end{bmatrix} = \begin{bmatrix} W'_{T,PE} \\ W'_{T,PH} \end{bmatrix} \quad (13)$$

$$inv\left(\begin{bmatrix} -a_{E,E} & -a_{E,H} \\ -a_{H,E} & -a_{H,H} \end{bmatrix} \right) = \begin{bmatrix} mia_{E,E} & mia_{E,H} \\ mia_{H,E} & mia_{H,H} \end{bmatrix} \quad (14)$$

$$\begin{bmatrix} P_E \\ P_H \end{bmatrix} = \begin{bmatrix} mia_{E,E} & mia_{E,H} \\ mia_{H,E} & mia_{H,H} \end{bmatrix} \begin{bmatrix} W'_{T,PE} \\ W'_{T,PH} \end{bmatrix} \quad (15)$$

Finally, the TP concentrations for the epilimnion (PE) and hypolimnion (PH) layers were calculated using the following equations (Equations 16-17):

$$P_E = mia_{E,E} \cdot W'_{T,PE} + mia_{E,H} \cdot W'_{T,PH} \quad (16)$$

$$P_H = mia_{H,E} \cdot W'_{T,PE} + mia_{H,H} \cdot W'_{T,PH} \quad (17)$$

The TP load is transported along the streams and enters the epilimnion layer of the lake due to density differences between the streams and the lake. The water densities of the streams in the basin were calculated using the equations provided by Millero and Poisson in 1981 (Table 3). For this purpose, the monthly average air temperatures for the period 2012-2022 from the Köyceğiz Station of the Turkish State Meteorological Service (TSMS) were used to calculate the stream water temperatures based on the relationship given by Stefan and Preud'homme 1993. It can be stated that a significant portion of the streams examined in the relevant reference has similar basin sizes and flow rates to the streams in the Köyceğiz Lake basin, and they also show similarities in terms of climate characteristics due to their latitude. The salinity level for the streams was assumed to be zero, and in order to stay on the most reliable side, it was assumed that there was no increase in stream water temperatures due to climate change. On the other hand, to determine the density of Köyceğiz Lake, the values for the lowest density of the lake given in August by Kazancı et al. 1992 were used, and the density of Köyceğiz Lake was calculated as 1000.36 kg m^{-3}. When considering this value in the context of current conditions and climate change, according to Mohamed et al. 2019, there was a temperature increase of 0.038 °C per year in surface seawater temperatures in the Levantine Basin between 1992 and 2018. Therefore, it can be said that the sea surface temperature in the region has increased by approximately 1 °C since 1992. When this increase is reflected in the lake water temperature, the density of the lake is calculated as 1000.045 kg m^{-3}. Consequently, the meromictic condition of Köyceğiz Lake remains unaffected by the increase in water temperature due to climate change and the resulting change in lake density.

Since total phosphorus is kinetically conservative, the only loss mechanisms are outflow (already obtained through the water balance) and settling velocity, which needs to be calibrated as a parameter. It is assumed that TP in the lake is transported solely through precipitation at different sedimentation rates in the epilimnion and hypolimnion.

The model was calibrated by comparing the model results with the surface and bottom layer TP concentrations measured in the monitoring study published by Keskin (2019). Model calibration was achieved by adjusting the settling rates of the epilimnion and hypolimnion compartments. A spreadsheet-based infrastructure was also developed for automatically generating nutrient loads, the lake eutrophication model, and its optimization-based calibration (Figure 5).

Model calibration was performed using nonlinear programming, where the objective was to minimise the difference between the model results and field data. Following the calibration of the model, a validation study was conducted for the epilimnion layer. It should be noted that the field data for the years 2008-2011, provided in Taşeli (2017), only pertained to the lake's surface water. The calculated total loads for 2008-2011 were utilised during the validation process.

Results and Discussion

Estimation of TP Loads

Diffuse and point source TP loads from various activities were estimated for 1990, 2000, 2006, 2012, and 2018 (Table 4).

The point source TP loads were regulated through the operation of municipal wastewater treatment plants starting in 2002. The total point source TP load was calculated as 2.47 tons per year in 2018, compared to 8.93 tons per year before the treatment plant became operational. Tanık et al. (2005) estimated the point source TP load of the lake as 1.88 tons per year in 2004. Despite the presence of the wastewater treatment plant, the increase in the TP load can be attributed to the growing population in the basin.

Diffuse pollution in the basin was assessed by considering TP loads originating from agricultural activities (fertiliser usage), livestock activities, and land use activities. To facilitate calibration, the results from 2006 can be compared to those obtained by Tanık et al. (2005). Their study determined the amount of diffuse pollution to be 26.4 tons of TP per year using the MONERIS (MOdelling Nutrient Emissions into RIver Systems) approach. It can be inferred that the unit loads and assumptions were adequately appropriate for the case area compared to the available literature.

Table 3. Estimated monthly densities of the stream's water

Months of the year	Monthly average T (°C)-air [a]	Monthly average T (°C) –water	Estimated density of the streams ϱ (kg m^{-3}) [c]
1	9.2	11.9	999.56
2	11.3	13.4	999.38
3	12.8	14.6	999.21
4	17.0	17.7	998.70
5	21.5	21.2	998.00
6	26.2	24.6	997.20
7	29.5	27.1	996.54
8	29.5	27.1	996.54
9	25.8	24.4	997.25
10	20.2	20.2	998.21
11	15.2	16.4	998.93
12	10.6	12.9	999.44

[a]: TSMS, Köyceğiz Station, monthly average air temperature data between 2012-2022.
[b]: Calculation based on Stefan and Preud'homme, 1993.
[c]: Calculation based on Millero and Poisson 1981.

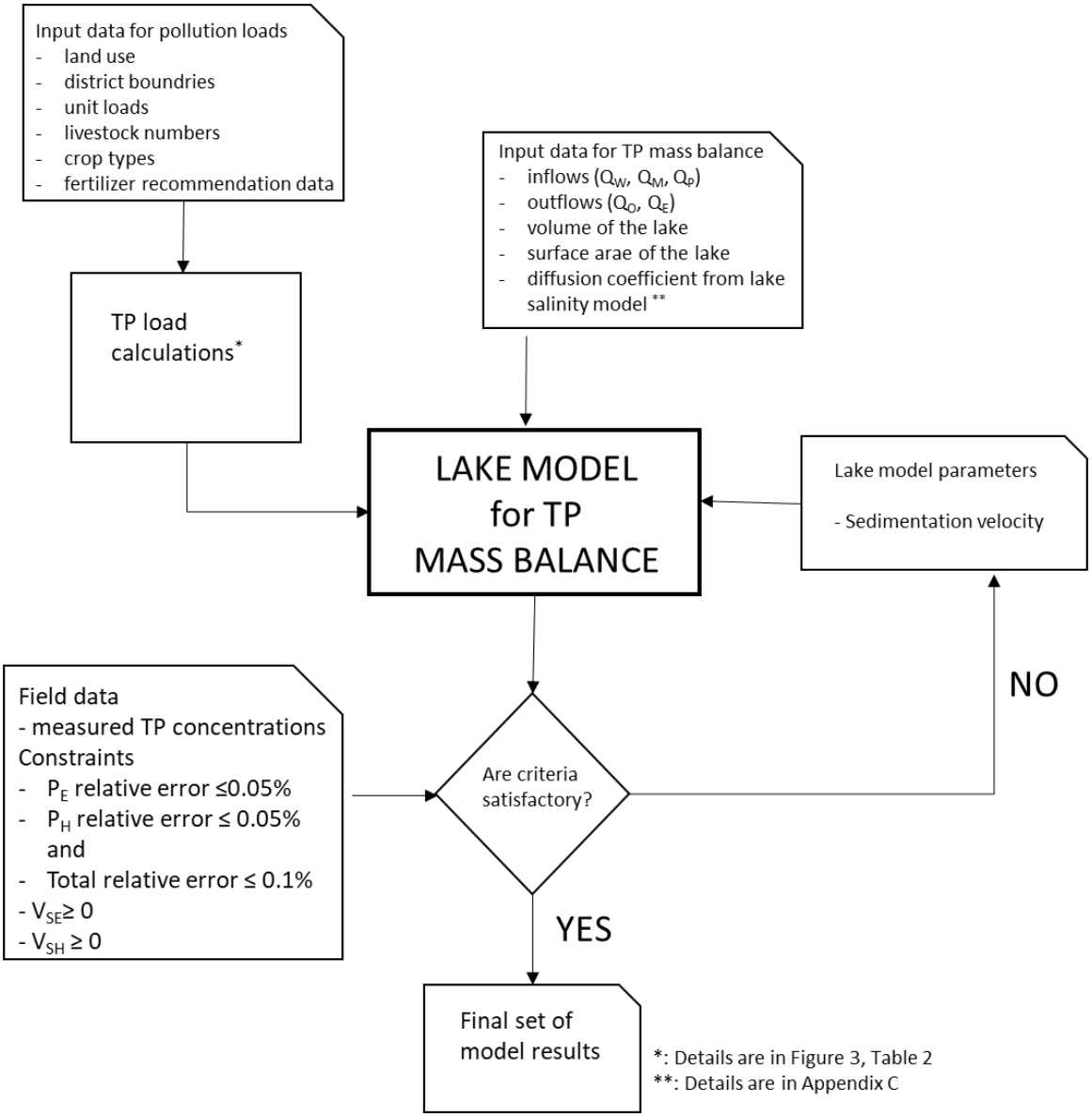

Figure 5. Flow chart of the optimisation of the lake model for TP mass balance

Table 4. Point and diffuse TP pollution loads reaching the lake (ton/yr)

Source Type	Diffuse Source TP Loads (ton/yr)			Point Source TP Load (ton/yr)	TP Load (ton/yr)		
Years	Land use Activity	Agricultural Activity	Livestock Activity	Domestic Wastewater Treatment Plant Discharge	Total Diffuse Source	Total Point Source	Total
1990	5.3	16.57	1.40	7.95	23.27	7.95	31.21
2000	5.3	16.70	3.30	8.93	25.33	8.93	34.26
2006	5.4	17.16	5.05	2.22	27.59	2.22	29.81
2012	5.4	17.16	6.00	2.28	28.56	2.28	30.84
2018	5.4	17.33	7.34	2.47	30.06	2.47	32.54

Considering the findings, when examining the diffuse source TP loads, it is evident that fertiliser usage (58%) and livestock activities (24%) had a significant impact in 2018. Evaluating the calculated diffuse source loads by year, it can be observed that the total diffuse TP loads exhibited an increasing trend.

Comparing the estimated diffuse nutrient loads in this study with the point sources, the results of the load calculations indicated that diffuse pollution accounted for 92% of the TP distribution in the basin. Diffuse source TP loads were considerably higher than the point source TP loads, which aligns with the distribution calculated by Tanık et al. (2005). Both studies emphasise that measures have been implemented to control point sources, achieve the desired water quality in the lake, and prevent eutrophication. However, insufficient actions have been taken since 2004 to reduce diffuse pollution, highlighting the need for additional measures.

Travel Time in The Streams

An investigation of the streams, based on flow data and topographical information (main streams with high slopes), revealed that the water travel time in the streams was mainly within a range of hours, rarely exceeding a day (Table 5). As a result, nutrient retention and transformation in the streams should have been addressed at this study stage. Furthermore, the streams were considered conduits that collect and channel the phosphorus loads into the basin.

The longest travel time, 8 hours, was observed along Namnam Creek, while the shortest travel time, 2 hours, was observed along Kargıcak Creek. Considering that over 50% of the basin area belongs to Namnam Creek and that a significant portion of the pollution loads originates from the Namnam Creek basin, TP is transported through the streams hourly. A similar approach was applied to modelling the basin in the study conducted by Tanık et al. (2005).

The Lake Eutrophication Model System

A simple model system based on the phosphorus budget in meromictic Köyceğiz Lake was successfully established and calibrated (Table 6). The model calibration involved comparing the yearly average TP concentrations in the epilimnion and hypolimnion with the surface and bottom monitoring results published by Keskin (2019). It was performed using an optimisation algorithm to minimise the steady-state model results disparity. The calibration yielded satisfactory results, with a total relative error of less than 1% for TP concentrations and a relative error of 0.5% for each layer's TP concentration. The calculated settling velocities were 0.092 and 0.005 for the epilimnion and hypolimnion layers, respectively.

The validation study results for the epilimnion indicate that the calculated TP concentration was 35.16 µg L^{-1}, while the measured concentration was 35.7 µg L^{-1} (Taşeli, 2017), averaging over four years. The model successfully estimated the TP concentration within a range of ±1-2% of the difference for the epilimnion.

According to the Surface Water Quality Regulations (SWQR) in Türkiye (MoAF, 2021) Annex-6, Table-9, if the Trophic State Index (TSI) of TP falls between 52 and 62, the lake is classified as eutrophic. Based on the model results, Köyceğiz Lake was eutrophic in both layers, with TSI (TP) values of 56 for the epilimnion and 70 for the hypolimnion.

Table 5. TP travel time in the main streams of the basin

	Length of creek (km)	Average width of the creek (m)	Average velocity (m s^{-1})	Average travel time (h)
Namnam Creek	54	25	1.88	8
Yuvarlak Creek	21	14	1.24	5
Kargıcak Creek	11	10	1.45	2
Sarıöz Creek	5	10	0.37	4
Hamitköy Creek	7	10	0.24	7

Future Assessment of Eutrophication

The model, at this stage, proved to be satisfactory for investigating and assessing the trophic state of Köyceğiz Lake in the future, considering various influencing factors such as changes in water budget due to climate change and alterations in total TP load resulting from developments in the basin, including population growth and expansion of the livestock sector.

Table 7 presents the estimated freshwater inflow from the basin into the lake and the point and diffuse TP loads. As observed in Table 7, while total TP loads are expected to exhibit a slight 4% increase due to anticipated developments in the basin, it is predicted that freshwater inflow will experience a significant decrease of 65% between 2018 and 2035, primarily attributed to the regional impacts of climate change. Looking ahead to the predicted changes between 2035 and 2095, total TP loads continue to rise by 8%, whereas freshwater inflow continues to decline by 28%.

When running the eutrophication model with the data provided in Table 7 for future projections, we obtained the yearly average concentrations of epilimnion TP (PE) and hypolimnion TP (PH) in the lake (Table 8). The model was executed for three scenarios: Scenario A, where only the freshwater inflow changes; Scenario B, where only the TP load changes; and Scenario C, where both freshwater inflow and TP loads change.

In Figure 6, the TSI results illustrating the future eutrophication status of the lake are presented for the epilimnion (a) and hypolimnion (b). Analysing the epilimnion situation between the 2030s and 2090s, the calculated TSI values of 66 and 68 in Scenario A and 57 and 58 in Scenario B indicate that the crucial factor determining the future eutrophication status in the lake basin is the reduction in freshwater inflow caused by climate change. Considering the combined impact in Scenario C, the projected TSI values of 67 and 70 indicate a hypertrophic status (TSI>62).

The findings indicate that the hypolimnion would exhibit a more severe hypertrophic status with significantly higher TSI values. Between the 2030s and 2090s, the calculated TSI values were 78 and 81 in Scenario A, 70.6 and 71.5 in Scenario B, and 79 and 82 in Scenario C, respectively. It was demonstrated that for both layers, the impact of climate change, specifically the reduction in freshwater inflow, had a more pronounced influence on the trophic state of Köyceğiz Lake compared to the developments in the basin and the resulting point and diffuse TP pollution.

Table 6. Model results

Parameters	Unit	Abbreviation	Model Result	Field Data
Inflow from the Mediterranean Sea	$m^3\ s^{-1}$	Q_M	2.63	-
Diffusive transport in the lake	$m^3\ s^{-1}$	$E_{E,H}$	7.50	-
Outflow	$m^3\ s^{-1}$	Q_O	28.06	-
Settling velocity in the epilimnion	$m\ d^{-1}$	$V_{S,E}$	0.028	-
Settling velocity in the hypolimnion	$m\ d^{-1}$	$V_{S,H}$	0.003	-
Total Phosphorus in the epilimnion	$\mu g\ L^{-1}$	P_E	37.52	37.5
Total Phosphorus in the hypolimnion	$\mu g\ L^{-1}$	P_H	97.45	97.5

Table 7. Future freshwater inflow and TP loads

Years	Freshwater Inflow ($m^3\ s^{-1}$)	Point TP Load (ton yr^{-1})	Diffuse TP Load (ton yr^{-1})
2030s	8.17	2.91	30.87
2040s	7.78	3.16	31.34
2050s	7.40	3.40	31.66
2060s	7.02	3.63	31.89
2070s	6.64	3.84	32.07
2080s	6.25	4.04	32.20
2090s	5.87	4.21	32.31

Table 8. Future average TP concentrations in Köyceğiz Lake for different scenarios

Years	Scenario A		Scenario B		Scenario C	
	P_E (µg L^{-1})	P_H (µg L^{-1})	P_E (µg L^{-1})	P_H (µg L^{-1})	P_E (µg L^{-1})	P_H (µg L^{-1})
2030s	71.62	173.11	38.78	100.26	75.56	184.05
2040s	75.93	182.65	39.51	101.87	79.96	191.60
2050s	77.84	186.89	40.08	103.13	83.15	198.67
2060s	79.85	191.35	40.54	104.16	86.29	205.63
2070s	81.96	196.04	40.94	105.04	89.43	212.62
2080s	84.25	201.12	41.27	105.78	92.68	219.82
2090s	86.61	206.35	41.56	106.41	95.93	227.03

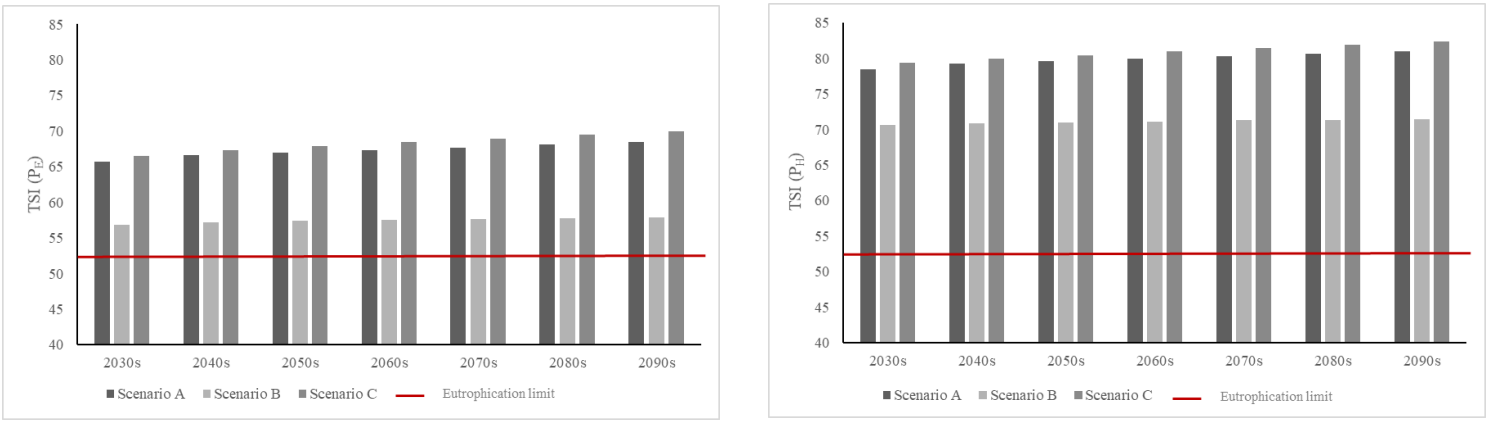

(a) (b)

Figure 6. Different scenarios TSI results for the epilimnion (a) and hypolimnion (b)

Conclusions

Köyceğiz Lake is at risk from two severe phenomena: (1) changes in freshwater inflow due to climate change, and (2) increasing agricultural and partially controlled livestock activities leading to diffuse pollution.

A successful model system has been developed and calibrated to assess the TP concentration in Köyceğiz Lake. The model provides results about future scenarios, including development and climate change. The eutrophication model results indicate that Köyceğiz Lake was already eutrophic in both layers in 2018. Given that Köyceğiz Lake is a designated environmental protection area, the objective should be to achieve a trophic status better than eutrophic, preferably mesotrophic (TSI (TP) < 52). However, the projected future situation suggests that the lake's trophic status will be hypertrophic. The model developed here is a simple model that requires fewer parameters to understand the key factors driving eutrophication in the lake.

Consequently, the model developed here can serve as a management tool for decision-makers to select appropriate measures in the basin to prevent eutrophication.

Compliance with Ethical Standards

Conflict of interest: The authors declare that they have no actual, potential, or perceived conflict of interest for this article.

Ethics committee approval: Ethics committee approval is not required for this study.

Funding disclosure: -

Acknowledgements: -

Disclosure: -

References

Ayaz, S., Aktaş, Ö., Dağlı, S., Aydöner, C., Aytış, E.A., Akça, L. (2013). Pollution loads and surface water quality in the Kızılırmak Basin, Turkey. *Desalination and Water Treatment*, 51(7-9), 1533-1542. https://doi.org/10.1080/19443994.2012.698814

Ayaz, S., Atasoy Aytış, E., Gürsoy Haksevenler, H., Koyunluoğlu Aynur, Ş., Dilaver, M., Erdoğan, N., Karaaslan, Y. (2021). An approach for determining the nutrient sensitive areas: a case study for Gediz River Basin, Turkey. *Environmental Monitoring and Assessment*, 193(5), 1-20. https://doi.org/10.1007/s10661-021-09017-x

Ayaz, S., Atasoy Aytış, E., Koyunluoğlu Aynur, Ş., Kıran, B., Beşiktaş, M., Sarıkaya, Ö., Karaaslan, Y. (2022). Simplified methodologies to designate sensitive areas and nitrate vulnerable zones: A case study of Yesilirmak River Basin, Turkey. *Environmental Quality Management*, 32(1), 483-494. https://doi.org/10.1002/tqem.21833

Ayaz, S., Aytis, E., Aynur, S., Haksevenler, B.H., Kiran, B., Dereli, E.M., Dilaver, M., Erdogan, N., Besiktas, M., Kinaci, C. (2017). The methodology of pollution load calculations. Solutions to Water Challenges in MENA Region, *Proceedings of the Regional Workshop, Cairo, Egypt*, April 25-30, Göttingen, Germany: Cuvillier Verlag.

Balooch, M.A. (2009). Hydrological simulation program-Fortran (HSPF) model as a decision support tool for a developing country-A case study from Turkey. [dissertation]: İTÜ.

Bayari, C. S., Kazanci, N., Koyuncu, H., Çağlar, S. S., Gökçe, D. (1995) Determination of the origin of the waters of Köyceğiz Lake, Turkey. *Journal of Hydrology*, 166(1-2), 171-191. https://doi.org/10.1016/0022-1694(94)02554-O

Buckley, C. and Carney, P. (2013). The potential to reduce the risk of diffuse pollution from agriculture while improving economic performance at farm level. *Environmental Science and Policy*, 25, 118-126. https://doi.org/10.1016/j.envsci.2012.10.002

Carlson, R.E. (1977). A trophic state index for lakes. *Limnology and Oceanography*, 22(2), 361-369. https://doi.org/10.4319/lo.1977.22.2.0361

Carlson, R.E., Simpson, J. (1996). A coordinator's guide to volunteer lake monitoring methods. *North American Lake Management Society*.

CORINE Land Cover. Copernicus, Available online: http://land.copernicus.eu/pan-european/corine-land-cover (accessed on 10 May 2022).

DEFRA (Department for Environment, Food and Rural Affairs) (2002). The Government's Strategic Review of diffuse water pollution from agriculture in England: Agriculture and Water: A Diffuse Pollution Review.

Ekdal, A. (2008). Water quality modeling of Köyceğiz-Dalyan Lagoon. [dissertation]: İTÜ.

Ertürk, A., Ekdal, A., Gürel, M., Karakaya, N., Güzel, Ç., Gönenç, İ.E. (2014). Evaluating the impact of climate change on groundwater resources in a small Mediterranean watershed. *Science of the Total Environment*, 499, 437-447. https://doi.org/10.1016/j.scitotenv.2014.07.001

Ertürk, A. (2002). Hydraulic modeling of Köyceğiz-Dalyan Lagoon system. [master's thesis]: İTÜ.

Görgüner, M., Kavvas, M.L, Ishida, K. (2019). Assessing the impacts of future climate change on the hydroclimatology of the Gediz Basin in Turkey by using dynamically downscaled CMIP5 projections. *Science of the Total Environment*, 648, 481-499. https://doi.org/10.1016/j.scitotenv.2018.08.167

Gürel, M., Erturk, A., Şeker, D.Z., Tanik, A., Ekdal, A., Avsar, C., Öztürk, İ. (2011). Estimation of monthly diffuse nutrient loads for a watershed in Turkey. *Water and Environment Journal*, 25(2), 219-229. https://doi.org/10.1111/j.1747-6593.2009.00214.x

Gürel, M. (2000). Nutrient dynamics in coastal lagoons: Dalyan Lagoon case study. [dissertation]: İTÜ.

Güzel, Ç. (2010). Application of SWAT model in a watershed in Turkey. [master's thesis]: İTÜ.

IPCC (2022). Sixth Assessment Report, Working Group II-Impacts, Adaptation and Vulnerability.

Karaca, T. (2020). Determination of some ecological parameters in Dalyan Channels (Köyceğiz-Muğla). [master's thesis]: Muğla Sıtkı Koçman University.

Kazanci, N., Plasa, R.H., Neubert, E., İzbirak, A. (1992). On the limnology of Lake Köycegiz (SW Anatolia). *Zoology in the Middle East*, 6(1), 109-126. https://doi.org/10.1080/09397140.1992.10637619

Keskin, F. (2019). Determination of toxic metal and eutrophication risks in Köyceğiz Lake Dalyan Lagoon system, Turkey. [dissertation]: Muğla Sıtkı Koçman University.

Koçak, M., Kubilay, N., Tuğrul, S., Mihalopoulos, N. (2010). Atmospheric nutrient inputs to the northern levantine basin from a long-term observation: sources and comparison with riverine inputs. *Biogeosciences*, 7(12), 4037-4050. https://doi.org/10.5194/bg-7-4037-2010

Kress, N., Herut, B. (2001). Spatial and seasonal evolution of dissolved oxygen and nutrients in the Southern Levantine Basin (Eastern Mediterranean Sea): chemical characterization of the water masses and inferences on the N: P ratios. *Deep Sea Research Part I: Oceanographic Research Papers*, 48(11), 2347-2372. https://doi.org/10.1016/S0967-0637(01)00022-X

Krom, M.D., Kress, N., Brenner, S., Gordon, L.I. (1991). Phosphorus limitation of primary productivity in the eastern Mediterranean Sea. *Limnology and Oceanography*, 36(3), 424-432. https://doi.org/10.4319/lo.1991.36.3.0424

Krom, M.D., Woodward, E.M. S., Herut, B., Kress, N., Carbo, P., Mantoura, R.F.C., Zodiatis, G. (2005). Nutrient cycling in the south east Levantine basin of the eastern Mediterranean: Results from a phosphorus starved system. *Deep Sea Research Part II: Topical Studies in Oceanography*, 52(22-23), 2879-2896. https://doi.org/10.1016/j.dsr2.2005.08.009

Lazzari, P., Solidoro, C., Salon, S., Bolzon, G. (2016). Spatial variability of phosphate and nitrate in the Mediterranean Sea: A modeling approach. *Deep Sea Research Part I: Oceanographic Research Papers*, 108,39-52. https://doi.org/10.1016/j.dsr.2015.12.006

Millero, F.J., Poisson, A. (1981). International one-atmosphere equation of state of seawater. *Deep Sea Research Part A. Oceanographic Research Papers*, 28(6), 625-629. https://doi.org/10.1016/0198-0149(81)90122-9

MoAF (2021). Implementing Regulation Amending the Regulation on Surface Water Quality, Turkish Official Gazette. 31513. Turkish.

MoAF (2018). Fertilizer Recommendation Guideline, Available on: https://www.tarimorman.gov.tr/TAGEM/Belgeler/yayin/TOPRAKSU%20G%C3%9CBRE%20TAVS%C4%B0YE%20%20Verileri.pdf (accessed on 10 May 2022).

Mohamed, B., Abdallah, A. M., Alam El-Din, K., Nagy, H., Shaltout, M. (2019). Inter-annual variability and trends of sea level and sea surface temperature in the Mediterranean Sea over the last 25 years. Pure and Applied Geophysics, 176, 3787-3810. https://doi.org/10.1007/s00024-019-02156-w

NAO (National Audit Office) (2010). Environment Agency, Tackling diffuse water pollution in England. https://doi.org/10.1111/j.1752-1688.1993.tb01502.x

Özgül, N. (2015). Determination of zooplankton fauna of Köyceğiz Lake (Muğla) and their relationship with physico-chemical properties. [dissertation]: Muğla Sıtkı Koçman University.

Stefan, H.G., Preud'homme, E.B. (1993). Stream temperature estimation from air temperature. *JAWRA Journal of the American Water Resources Association*, 29(1), 27-45.

Şen, O.L. (2013). A holistic view of climate change and its impacts in Turkey. Istanbul Policy Center, Sabancı University, Stiftung Mercator Initiative, Mercator-IPC Fellowship Project, Istanbul, Turkey.

Şen, Z. (2020). Water structures and climate change impact: a review. *Water Resources Management*, 34(13), 4197-4216. https://doi.org/10.1007/s11269-020-02665-7

Tanık, A., Seker, D.Z., Gürel, M., Adalı, I., Ertürk, A., Ekdal, A. (2005). Results of nutrient emission modeling in a watershed-application of the MONERIS Model. Proceedings of the Management of Residues Emanating from Water and Wastewater Treatment, Johannesburg, South Africa, 9-12 August.

Taşeli, B.K. (2017). Influence of channel traffic and Koycegiz Lake on the water quality of Dalyan Channel network. *Environmental Engineering & Management Journal (EEMJ)*, 16(12).

TSMS, Turkish State Meteorologic Servise; Köyceğiz Station, air temperature data, 2012-2022.

TurkStat (a). Turkish Statistical Institute, Population, and demography statistics, Available online: https://biruni.tuik.gov.tr/medas/?kn=101&locale=tr (accessed on 10 May 2022).

TurkStat (b). Turkish Statistical Institute, Agriculture statistics, Available online: https://biruni.tuik.gov.tr/medas/?kn=101&locale=tr (accessed on 10 May 2022).

Udias, A., Malagò, A., Pastori, M., Vigiak, O., Reynaud, A., Elorza, F.J., Bouraoui, F. (2016). Identifying efficient nitrate reduction strategies in the Upper Danube. *Water*, 8(9), 371. https://doi.org/10.3390/w8090371

Vollenweider, R.A. (1976). Advances in defining critical loading levels for phosphorus in lake eutrophication. *Mem. 1st ital. Idrobiol,* 33, 53-58.

Appendix A

Estimation of Future Population and Livestock

To estimate the population, number of bovine livestock and ovine livestock in the watershed, the logistic curve method was used (Eq A.1).

$$\frac{dN}{dt} = r \cdot N \cdot \left(1 - \frac{N}{K}\right) \tag{A.1}$$

where N is the number of variable of interest (population, number of bovine livestock and number of ovine livestock), t is the time, r is the increase rate constant (1/time) and K is the quantity in numbers related to the variable of interest at saturation (acting like a carrying capacity). Evaluation of Equation A.1 leads to a Bernoulli type of differential equation;

$$\frac{dN}{dt} = r \cdot N - r \cdot N \cdot \frac{N}{K} \tag{A.2}$$

$$\frac{dN}{dt} = r \cdot N - \frac{r}{K} \cdot N^2 \tag{A.3}$$

$$\frac{dN}{dt} - r \cdot N = -\frac{r}{K} \cdot N^2 \tag{A.4}$$

which can be solved for the initial condition (t=0, N=N_0). Setting an integration as given in Equation A.5, the general solution is as given in Equation A.7.

$$I(t) = exp\left((1-2) \cdot \int -r \cdot dt\right) = exp\left(-1 \cdot \int -r \cdot dt\right) = exp\left(1 \cdot r \cdot \int dt\right) = exp(r \cdot t) \tag{A.5}$$

$$N^{-1} = \frac{1}{I(t)} \cdot \left(-\int \left(-\frac{r}{K} \cdot I(t)\right) \cdot dt + S\right) = \frac{1}{exp(r \cdot t)} \cdot \left(-\int \left(-\frac{r}{K} \cdot exp(r \cdot t)\right) \cdot dt + S\right) =$$

$$\frac{1}{exp(r \cdot t)} \cdot \left(\frac{r}{K} \cdot \int \left(exp(r \cdot t)\right) \cdot dt + S\right) = \frac{1}{exp(r \cdot t)} \cdot \left(\frac{r}{K} \cdot \frac{exp(r \cdot t)}{r} + S\right)$$

$$\frac{1}{exp(r \cdot t)} \cdot \frac{r}{K} \cdot \frac{exp(r \cdot t)}{r} + \frac{S}{exp(r \cdot t)} = \frac{1}{K} + \frac{S}{exp(r \cdot t)} \tag{A.6}$$

$$(N^{-1})^{-1} = \left(\frac{1}{K} + \frac{S}{exp(r \cdot t)}\right)^{-1} = N = \frac{1}{\frac{1}{K} + \frac{S}{exp(r \cdot t)}} \tag{A.7}$$

where S is the integration constant to be determined using the initial conditions (Equation A.8 - Equation A.12).

$$N_0 = \frac{1}{\frac{1}{K} + \frac{S}{exp(r \cdot 0)}} = \frac{1}{\frac{1}{K} + S} \tag{A.8}$$

$$N_0 \cdot \left(\frac{1}{K} + S\right) = 1 \tag{A.9}$$

$$\frac{N_0}{K} + N_0 \cdot S = 1 \tag{A.10}$$

$$N_0 \cdot S = 1 - \frac{N_0}{K} \tag{A.11}$$

$$S = \frac{1 - \frac{N_0}{K}}{N_0} = \frac{1}{N_0} - \frac{N_0}{N_0 \cdot K} = \frac{1}{N_0} - \frac{1}{K} \tag{A.12}$$

Substituting the right side of Equation A.12 into Equation A.7 (Equation A.13) yields the desired solution N as a function of time (Equation A.14);

$$N = \frac{1}{\frac{1}{K} + \frac{S}{exp(r \cdot t)}} = N = \frac{1}{\frac{1}{K} + \frac{\frac{1}{N_0} - \frac{1}{K}}{exp(r \cdot t)}} \tag{A.13}$$

$$N(t) = \frac{1}{\frac{exp(r \cdot t)}{K \cdot exp(r \cdot t)} + \frac{\frac{K}{N_0} - 1}{K \cdot exp(r \cdot t)}} \tag{A.14}$$

$$= \frac{1}{\frac{exp(r \cdot t) + \frac{K}{N_0} - 1}{K \cdot exp(r \cdot t)}}$$

$$= \frac{K \cdot exp(r \cdot t)}{exp(r \cdot t) + \frac{K}{N_0} - 1}$$

$$N(t) = \frac{K \cdot exp(r \cdot t)}{exp(r \cdot t) + \frac{K}{N_0} - 1} \tag{A(15)}$$

Equation A.15 has two parameters (r,K) to be adjusted for the desired variable. For the adjustment of parameters, Excel solver (option non-linear gradient programming) was used where the sum of the absolute values of the differences between the estimated values of the variables by Equation A.15 and the data served as the goal function to be minimized.

To adjust (r,K) for the population, data in Table A.1 was used. The details of parameter adjustments and the estimations are given Table A.2, the goodness of fit with the population data is given Figure A.1 and the future estimate of population is given Figure A.2. For population, r was adjusted as 0.0193 where K was adjusted ad 80830.

Table A.1 Population data

Year	Population (person)
1990	27213
2000	30595
2006	33723
2008	33873
2009	34160
2011	34524
2012	34723
2018	37618
2020	39178

Table A.2 Intermediate results for population logistic-curve parameter adjustment

Year	Years passed from initial year (1990)	Population (person)	Estimated population (person)	Relative error
1990	0	27213	-	-
2000	10	30595	30793	0.006479063
2006	16	33723	33025	0.020691423
2008	18	33873	33780	0.002731337
2009	19	34160	34160	1.75216E-06
2011	21	34524	34922	0.011533759
2012	22	34723	35305	0.016756951
2018	28	37618	37618	2.93564E-07
2020	30	39178	38394	0.020012608

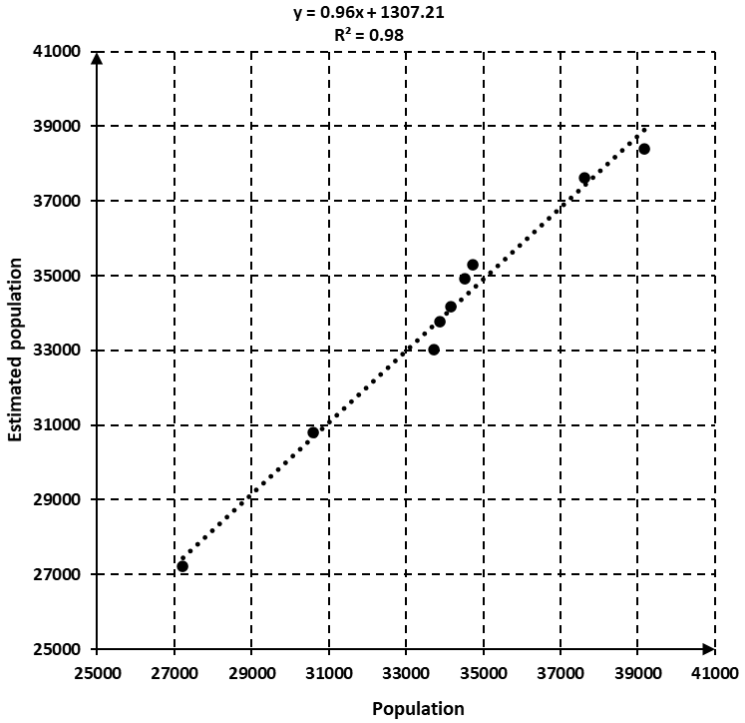

Figure A.1 Goodness of fit of the adjusted parameters r and K for population

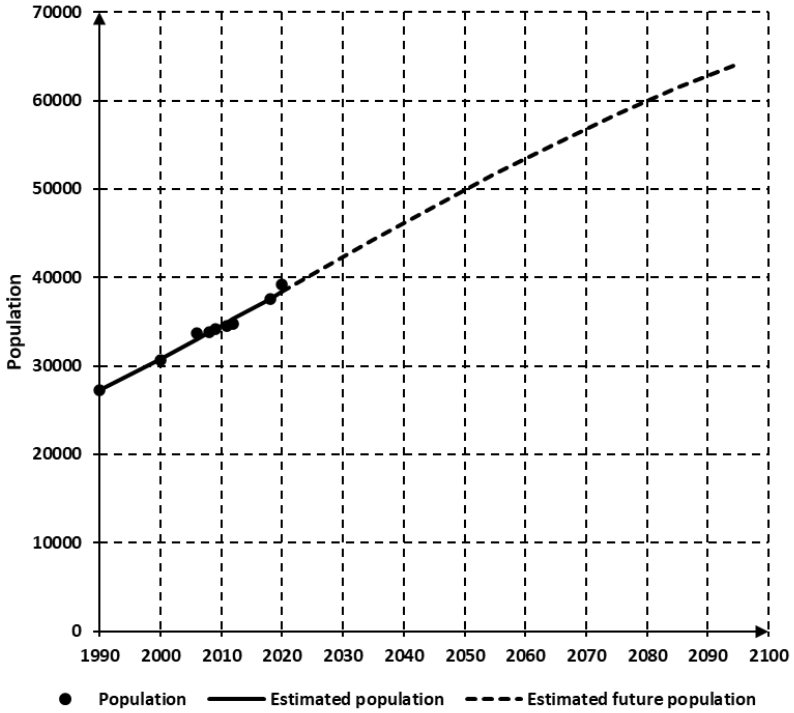

Figure A.2 Estimated population for the future

To adjust (r, K) for the bovine livestock, data in Table A.3 was used. The details of parameter adjustments and the estimations are given Table A.4, the goodness of fit with the bovine livestock data is given Figure A.3 and the future estimate of bovine livestock is given Figure A.4. For bovine livestock, r was adjusted as 0.0753 where K was adjusted ad 17045.

Table A.3 Bovine livestock data

Year	Bovine livestock
2004	9062
2005	9098
2006	10044
2007	9435
2008	10289
2009	10719
2010	10811
2011	11210
2012	11883
2013	13404
2014	12091
2015	11890
2016	12847
2017	12505
2018	14490
2019	13268
2020	14181
2021	12745

Table A.4 Intermediate results for bovine livestock logistic-curve parameter adjustment

Year	Years passed from initial year (2004)	Bovine livestock	Estimated Bovine livestock	Relative error
2004	0	9062	9062	-
2005	1	9098	9381	0.031125673
2006	2	10044	9697	0.034522646
2007	3	9435	10010	0.06091739
2008	4	10289	10319	0.002969657
2009	5	10719	10623	0.008925944
2010	6	10811	10922	0.010258963
2011	7	11210	11214	0.000304194
2012	8	11883	11499	0.032299272
2013	9	13404	11777	0.121408298
2014	10	12091	12047	0.003612329
2015	11	11890	12309	0.035209079
2016	12	12847	12562	0.022176758
2017	13	12505	12806	0.024080456
2018	14	14490	13042	0.099979941
2019	15	13268	13268	2.52913E-07
2020	16	14181	13484	0.049100834
2021	17	12745	13692	0.074313729

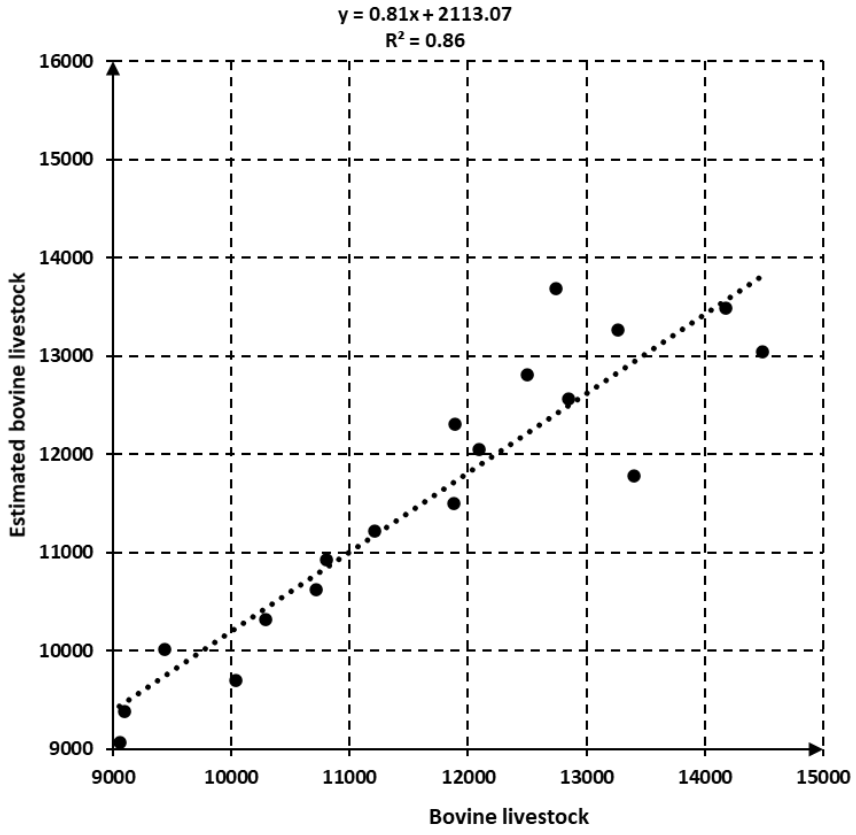

Figure A.3 Goodness of fit of the adjusted parameters r and K for bovine livestock

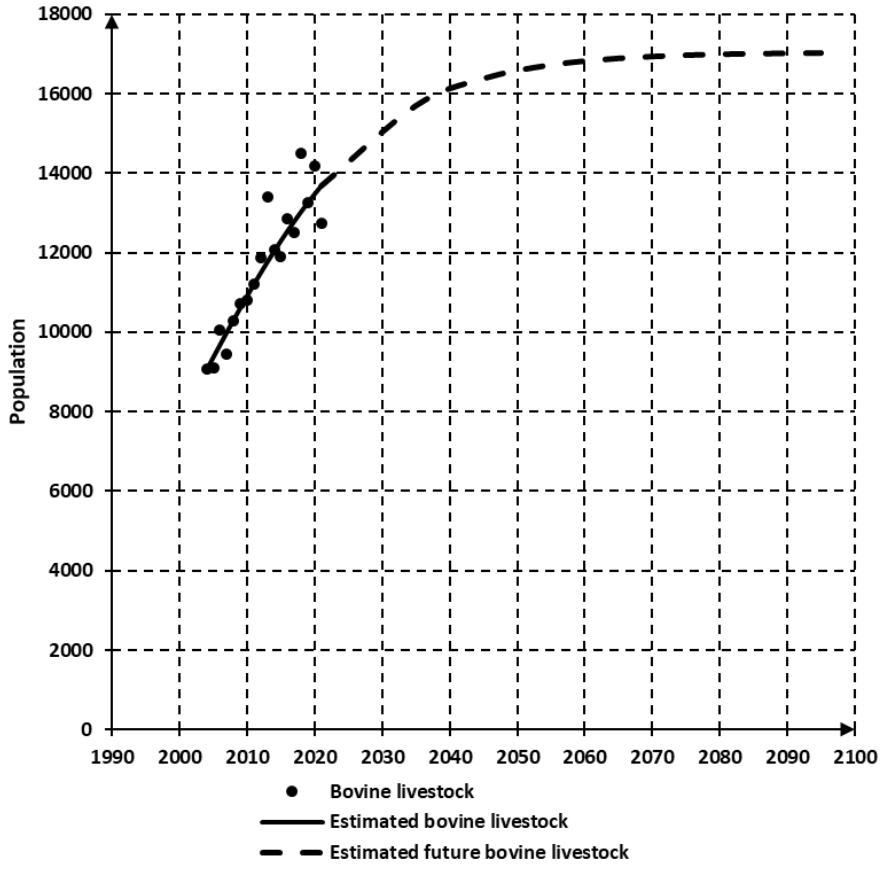

Figure A.4 Estimated population for the bovine livestock

To adjust (r, K) for the ovine livestock, data in Table A.5 was used. The details of parameter adjustments and the estimations are given Table A.6, the goodness of fit with the bovine livestock data is given in Figure A.5, and the future estimate of bovine livestock is given Fin igure A.6. For bovine livestock, r was adjusted as 0.0309 where K was adjusted ad 87308.

Table A.5 Ovine livestock data

Year	Ovine livestock
2004	20892
2005	17937
2006	19038
2007	18481
2008	18271
2009	18512
2010	18708
2011	22046
2012	23470
2013	27754
2014	33627
2015	27802
2016	31640
2017	24649
2018	29310
2019	27891
2020	32098
2021	30317

Table A.6 Intermediate results for ovine livestock logistic-curve parameter adjustment

Year	Years passed from the initial year (2004)	Ovine livestock	Estimated ovine livestock	Relative error
2004	0	20892	20892	-
2005	1	17937	21387	0.192366723
2006	2	19038	21890	0.14977748
2007	3	18481	22401	0.212062638
2008	4	18271	22919	0.254388968
2009	5	18512	23445	0.266501626
2010	6	18708	23979	0.281767
2011	7	22046	24521	0.112222723
2012	8	23470	25069	0.068121318
2013	9	27754	25625	0.076695595
2014	10	33627	26188	0.221212947
2015	11	27802	26758	0.037548311
2016	12	31640	27335	0.13606299
2017	13	24649	27919	0.132660826
2018	14	29310	28509	0.027322236
2019	15	27891	29106	0.043549127
2020	16	32098	29708	0.074453975
2021	17	30317	30317	3.11915E-09

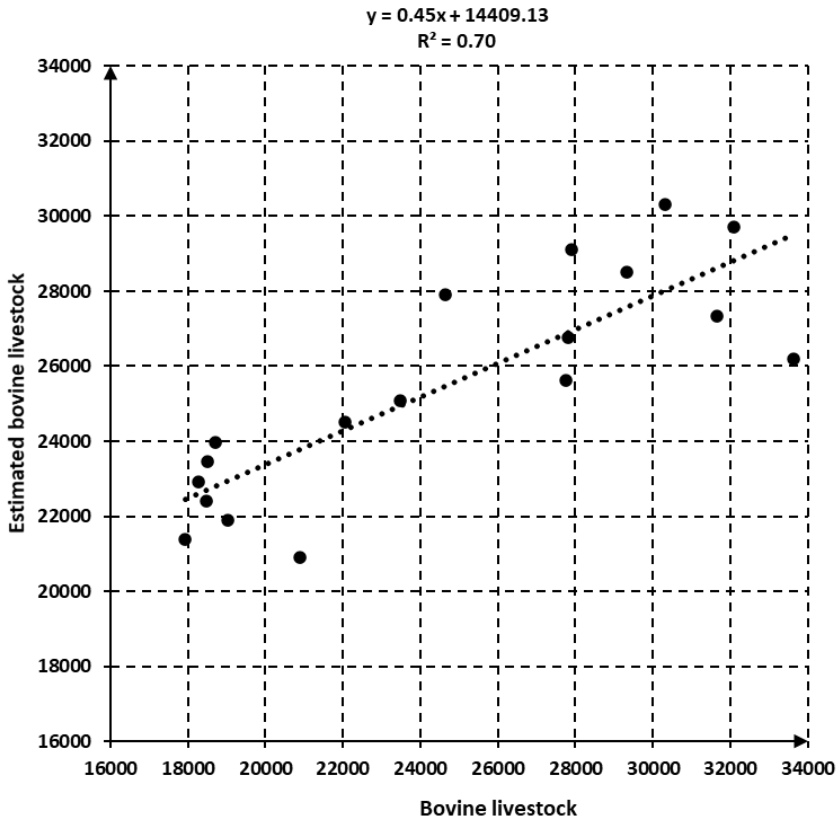

Figure A.5 Goodness of fit of the adjusted parameters r and K for ovine livestock

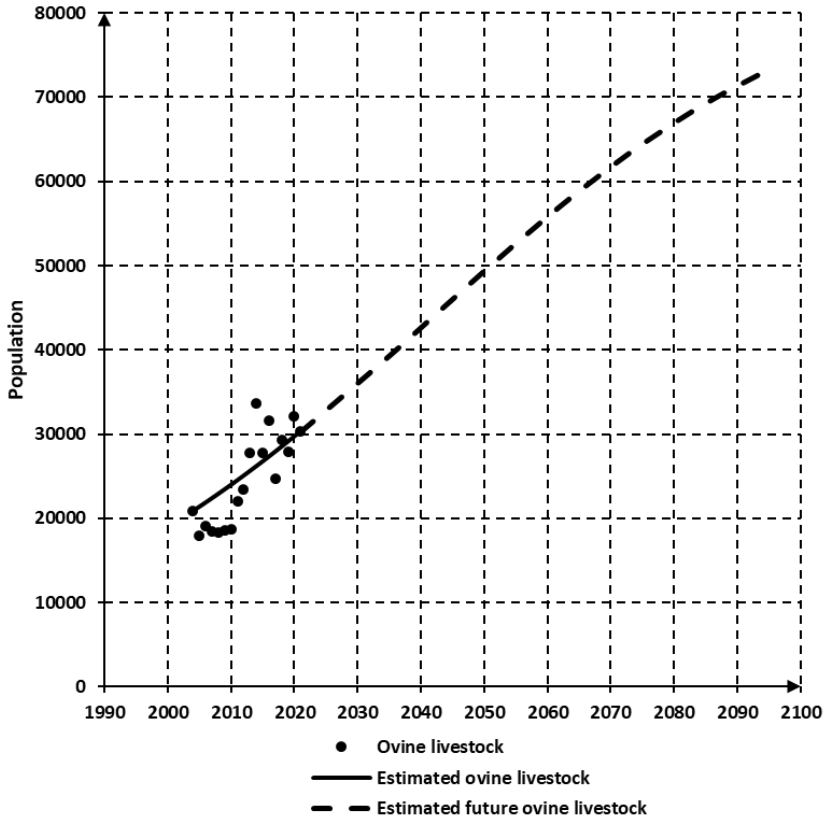

Figure A.6 Estimated population for the ovine livestock

Estimated population, bovine livestock and ovine livestock for the future are given in tables A.7, A.8 and A.9, respectively

Table A.7 Estimated population for the future

Year	Population
2035 (representing 2030's)	44221
2045 (representing 2040's)	48034
2055 (representing 2050's)	51711
2065 (representing 2060's)	55196
2075 (representing 2070's)	58444
2085 (representing 2080's)	61426
2095 (representing 2090's)	64124

Table A.8 Estimated bovine livestock for the future

Year	Bovine livestock
2035 (representing 2030's)	15705
2045 (representing 2040's)	16386
2055 (representing 2050's)	16728
2065 (representing 2060's)	16894
2075 (representing 2070's)	16973
2085 (representing 2080's)	17011
2095 (representing 2090's)	17029

Table A.9 Estimated ovine livestock for the future

Year	Ovine livestock
2035 (representing 2030's)	39335
2045 (representing 2040's)	46065
2055 (representing 2050's)	52681
2065 (representing 2060's)	58890
2075 (representing 2070's)	64469
2085 (representing 2080's)	69288
2095 (representing 2090's)	73311

Appendix B

Travel time in the streams

Manning equation is given in Equation B.1

$$\vartheta = \frac{\sqrt{J}}{n} \cdot R^{\frac{2}{3}} \quad \text{(B.1)}$$

$$Q = \frac{\sqrt{J}}{n} \cdot R^{\frac{2}{3}} \cdot A \quad \text{(B.2)}$$

where ϑ= cross-sectional average velocity (ms^{-1}), J= slope, R= hydraulic radius (m), Q= Flow of the stream (m^3s^{-1}), A= cross-sectional area (m^2), n= Manning's Roughness Coefficient.

$$Q = \frac{\sqrt{J}}{n} \cdot R^{\frac{2}{3}} \cdot D \cdot W \quad \text{(B.3)}$$

$$R = \frac{A}{P} \quad \text{(B.4)}$$

$$R = \frac{W \cdot D}{W + 2D} \quad \text{(B.5)}$$

$$D \ll W \quad \text{(B.6)}$$

$$W + 2D \sim W \quad \text{(B.7)}$$

$$R = \frac{W \cdot D}{W} \approx D \quad \text{(B.8)}$$

$$R = D \quad \text{(B.9)}$$

$$\frac{Q}{W} = \frac{\sqrt{J}}{n} \cdot D^{\frac{2}{3}} \cdot D \quad \text{(B.10)}$$

$$\frac{Q}{W} = \frac{\sqrt{J}}{n} \cdot D^{\frac{5}{3}} \quad \text{(B.11)}$$

The depth of the water channel (D) is considered much less than the width of the water channel (W) (Equation B.4-6), and the hydraulic radius is approximated by the depth of the water channel (Equation B.7-9). The Manning equation was applied by accepting that the roughness coefficient n was constant (n=0.035 for natural streams) and did not change along the stream. Using Equation B.10 results in the depth of the water channel (Equation B.11); subsequently, all these equations were substituted in Equation B.1, and the final equation to calculate the stream's average velocity (m·s-1) was obtained.

Appendix C

Salt Mass Balance

It has been accepted that there is only diffusion in terms of transport mechanism, the Mediterranean Sea water entering the hypolimnion layer comes out of the epilimnion layer, and yearly average evaporation and precipitation is equal in the lake.

The salinity of the Mediterranean Sea (S_M) at the lake's entrance was taken as 30 ppt [1]. While the average salinity of the lake at the epilimnion (S_E) is 3 ppt, it is 10 ppt at the hypolimnion (S_H).

Defining the terms as Q_W= Total inflow from the basin (m^3d^{-1}), Q_P= Flow from precipitation (m^3d^{-1}), Q_E= Flow from evaporation (m^3d^{-1}), Q_M= inflow from Mediterranean Sea (m^3d^{-1}), Q_O= Total outflow from the basin (m^3d^{-1}), S_E= Salinity of the epilimnion (ppt), S_H=Salinity of the hypolimnion (ppt), S_M=Salinity of the Mediterranean Sea (ppt), $E_{E,H}$= Diffusion from hypolimnion to epilimnion (m^3d^{-1}), Equations C.1 to 10 are written;

$$Q'_O = Q_W + Q_P - Q_E \quad \text{(C.1)}$$

$$Q_O = Q'_O + Q_M \quad \text{(C.2)}$$

$$Q_O = Q_W + Q_P - Q_E + Q_M \quad \text{(C.3)}$$

$$\frac{dS_E}{dt} = Q_M \cdot S_H - Q_O \cdot S_E + E_{E,H} \cdot (S_H - S_E) \quad \text{(C.4)}$$

$$\frac{dS_H}{dt} = Q_M \cdot S_M - Q_M \cdot S_H + E_{E,H} \cdot (S_E - S_H) \quad \text{(C.5)}$$

$$Q_M \cdot S_H - Q'_O \cdot S_E - Q_M \cdot S_E + E_{E,H} \cdot (S_H - S_E) = 0 \quad \text{(C.6)}$$

$$(S_H - S_E) \cdot Q_M + (S_H - S_E) \cdot E_{E,H} = Q'_O \cdot S_E \quad \text{(C.7)}$$

$$(S_M - S_H) \cdot Q_M + (S_E - S_H) \cdot E_{E,H} = 0 \quad \text{(C.8)}$$

$$(S_M - S_H) \cdot Q_M = (S_H - S_E) \cdot E_{E,H} \quad \text{(C.9)}$$

$$E_{E,H} = \frac{S_M - S_H}{S_H - S_E} \cdot Q_M \quad \text{(C.10)}$$

[1] Gürel, M. (2000). Nutrient dynamics in coastal lagoons: Dalyan Lagoon case study. [dissertation]: İTÜ.